May 2023

MAX VENTUS

Turbine Design Report

James Madison University
Collegiate Wind Competition 2023

Prototype Development Team

Nicholas Gartner	Prototype Development Lead; Blades Team	gartnenf@dukes.jmu.edu
Alexander Ziemke	Generator Team/Structure Team	ziemkeaj@dukes.jmu.edu
Joseph Sculley	Structural Foundation Team	scullyjd@dukes.jmu.edu
Jack Williams	Generator/Nacelle Team	will25jc@dukes.jmu.edu
Yazeed Salameh	Blades Team	salameys@dukes.jmu.edu
Austin Zicafoose	Electronics/Controls Team; Structural Foundation Team	zicafoab@dukes.jmu.edu
Mary Wari	Generator Team	warime@dukes.jmu.edu
Brandon Landes	Blades Team	landesbd@dukes.jmu.edu
Josh Savage	Electronics/Controls Team	savagejw@dukes.jmu.edu

Faculty Advisors

Dr. Keith Holland	Professor of Engineering
Dr. Jonathan Miles	Professor of Integrated Science and Technology

JMU
JAMES MADISON UNIVERSITY

COLLEGIATE WIND COMPETITION
U.S. DEPARTMENT OF ENERGY

Table of Contents

1. Executive Summary

The current James Madison University (JMU) prototype development team, the MaxVentus Collective, identified three areas of focus for improving the 2021-2022 teams' design. These foci included (1) enhancing the sand bed anchoring force, (2) reducing friction on the drivetrain, and (3) increasing the aerodynamics of the nacelle. The MaxVentus team has built upon the 2022 team's design and made iterations following the CWC 2023 Rules and Regulations (R&R).

Design concepts resulted from benchmarking of prior competition teams' reports, classroom learning, and literature review. A direct drive, horizontal axis rotor, with a three-blade configuration featuring an active pitch mechanism, was selected as the final rotor design. An SA7024 root airfoil profile and a Wortmann FX 60-100 tip airfoil were selected for the blade design. Airfoil chord lengths and twist angles were optimized for a tip-speed ratio (TSR) of 3.0. Blades were modeled in SolidWorks and 3D-printed using Onyx™ filament, a nylon and carbon fiber composite that provides flexibility and strength. A custom active pitching mechanism developed by the JMU 2022 team was modified to reduce friction on the drivetrain. Rotational energy from the rotor is converted to electrical energy by a direct drive, 3-phase, permanent magnet axial flux generator. The stator contains 9 hand-wound coils, each comprising 175 turns of 26 gauge wire. This design was selected based on extensive modeling to match the rotor torque and rotational speed characteristics with those of the generator under various electrical loads to maximize power output at various wind speed ranges based on the 2023 R&R. The generator design was validated by comparing actual against simulated power outputs at varying torques.

The foundation is comprised of a 25.40cm x 25.40cm (10in x 10in) steel tamper head used as the foundational plate, four 13.34cm modified hollow steel pipes with outer diameters of 4.94cm and inner diameters of 3.90cm used as the anchoring piles, and one other 9.00cm steel pipe with an outer diameter of 1.91cm and a 0.25cm thick wall used as the lower tower and adapting facet for the Organizer-provided Transition Piece (OPTP). These components were welded together to construct MaxVentus' foundation and anchoring system. Above the OPTP, the structural components that would be inside the wind tunnel are all made of 6061 aluminum, excluding the wind sensor mount and nacelle cover which both were 3D printed. Connected to the OPTP by three bolts is a base plate and tower sleeve securing a 54.45cm hollow pipe with an outer diameter of 3.81 and an inner diameter of 3.77cm used as the upper tower. The nacelle is supported and rotated by a flange that has been welded to the upper tower's top, effectively positioning the rotor hub at a height of 60cm from the base of the wind tunnel. After installation, the rotor can be aligned with the upwind direction and secured in place. Subsequently, a secondary plate below the flange and the nacelle's bottom plate generate a compressive force on the flange when fastened with three screws.

The electronics and control subsystem receives unregulated power from the generator, regulates and distributes that power. Power from the axial flux generator is regulated using a wide range buck booster and Schottky diode bridge to rectify the power to 12 volts DC. After the power has been rectified and regulated it is distributed throughout the system and to the load. The load is controlled through our control algorithm developed in Arduino IDE. The control algorithm is designed to maximize power by increasing the load with sensed wind speed between 5 and 11 m/s. Once the turbine detects wind speeds between 11 and 22 m/s the control algorithm will pitch the blades in order to maintain rated power output.

This report details the MaxVentus team's design decisions and results for the three main subsystems: Rotor, Structure, and Electronics/Controls. A fully functional wind turbine prototype was successfully fabricated, as shown in Figure 1.

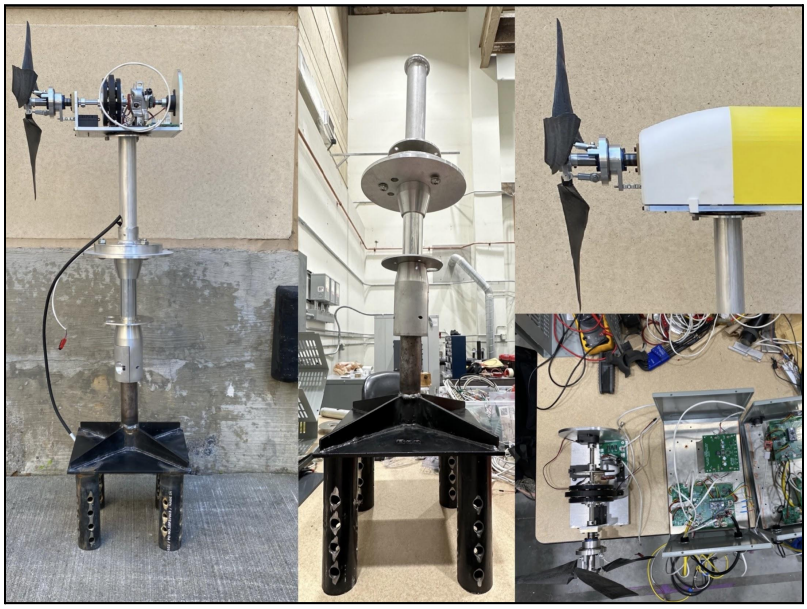

Figure 1: Fully Functional Assembled Wind Turbine Alongside the Subassemblies

2. Design Objectives

The MaxVentus team had three primary design objectives for the 2023 CWC, namely to enhance the design weaknesses observed in the 2022 JMU team's design. The three objectives included (1) strengthening the sand bed foundation system, (2) reducing friction on the drivetrain caused by a linear bearing of the blade pitch mechanism, and (3) improving the aerodynamics of the nacelle.

Among these objectives, the offshore foundation was identified as the most significant area in need of design improvement. During testing, the 2022 JMU team's foundation design shifted beyond competition allowances due to rotor thrust forces at high wind speeds. As described in subsequent sections, a more robust four-pile anchoring system was designed to resist the anticipated overturning moment and nacelle vibrations. To minimize the drivetrain and linear bearing friction, the team created a stainless steel sleeve that eliminated contact between the drivetrain and the pitching mechanism. Finally, to address the aerodynamics of the nacelle, a 3-D printed shell was designed to replace a flat aluminum front plate, resulting in a $9in^2$ reduction in the flat surface area at the front of the nacelle. These modifications resulted in significant improvements to the overall performance of the MaxVentus team's wind turbine design.

3. Rotor Design

The rotor blade designs were extensively modeled within QBlade and airfoils were acquired through an online database to be best optimized for wind speeds between 5-11 m/s.

Fabrication of all components of the rotor was completed in-house within JMU facilities. Testing of all rotor components occurred within JMU's wind tunnel and laboratory spaces.

3.1. Rotor and Blade Design

A three-blade, direct drive, horizontal axis rotor configuration was identified as the optimal rotor configuration based on benchmarking, estimation of power production potential, and rotational balance to reduce vibrations. Other configurations including more than three blades were not pursued due to the increased weight and material cost.

Promising airfoil profiles were researched and cataloged from prior competition reports as well as online databases with special attention to airfoils with high glide ratios (C_l/C_d) in low Reynolds number flows and high camber. Candidate blades constructed from these identified airfoils were then simulated in QBlade to compare power coefficient (C_p), torque, and rotational speed characteristics. Final blade designs were selected to maximize C_p and torque while producing significant torque at low wind speeds for cut-in.

Through this process, a blended blade consisting of a Wortmann FX 60-100 airfoil tip and an SA7024 root, shown in Figure 2, was selected. Chord lengths and twist angles were optimized for a TSR of 3.0, allowing for the necessary torque to drive the generator while limiting rotational speeds to approximately 1,500 RPM to manage the centripetal forces acting upon the blades and rotor. As shown in Figure 3, this design achieved a simulated C_p of 0.40 at a TSR of 3.0.

Figure 4 shows the selected blade's simulated power production at 0° pitch. At 11 m/s wind speeds, the rotor design is projected to generate approximately 45 W.

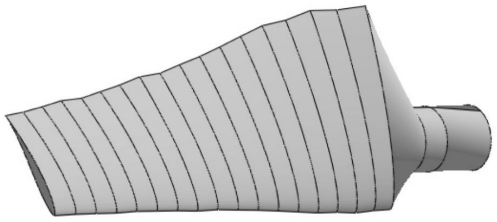

Pos (m)	Chord (m)	Twist	Foil
0	0.025	0	Circular Foil
0.03	0.025	0	Circular Foil
0.05	0.0778149	31.6737	SA7024
0.07	0.0768312	24.9296	SA7024
0.09	0.0725245	20.0535	SA7024
0.11	0.0655088	16.1663	SA7024
0.13	0.0597784	13.2495	SA7024
0.15	0.0564505	10.9908	FX60-100
0.17	0.0518555	9.19525	FX60-100
0.19	0.049563	8.23627	FX60-100
0.21	0.0459511	9.02881	FX60-100

Figure 2: CAD Image of Chosen Blade Design and List of Airfoil Segments

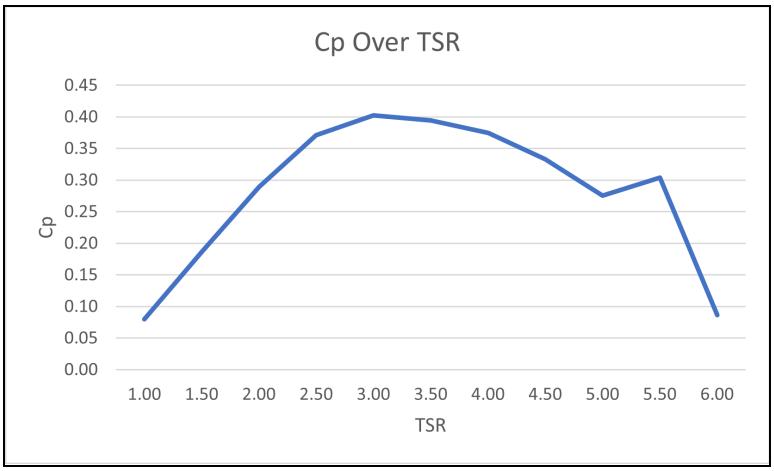

Figure 3: CP vs. TSR for chosen blades highlighting a Cp of ~0.4 at a TSR of 3

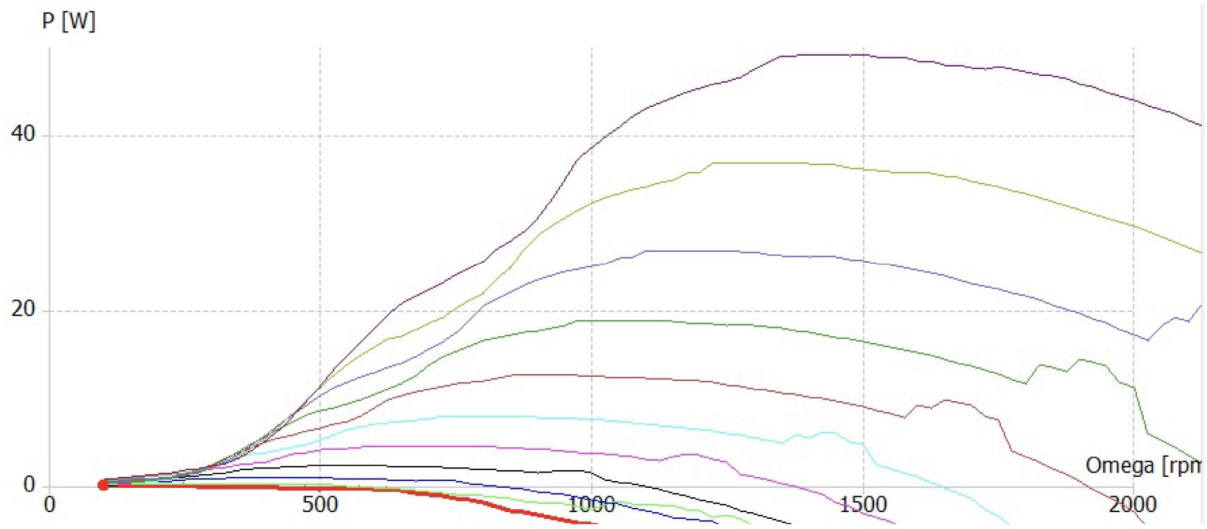

Figure 4: Power Production of Selected Blade

Following simulation and selection, the blade was modeled in SOLIDWORKS and 3-D printed using the Onyx™ filament, a carbon-fiber and nylon composite used by prior JMU teams. Upon finalizing the blade design and fabrication, the team performed deflection and load testing on the blades to determine their strength and durability. Simulations and past competitions indicated that blades would be subjected to a maximum thrust force of 10 N, and any deflection exceeding 5 inches would result in a collision with the nacelle or tower, a condition of failure. The load testing, shown in Figure 5, revealed that the blades can withstand up to 25 lbs (111 N) before reaching the deflection threshold, providing a thrust safety factor of 11.

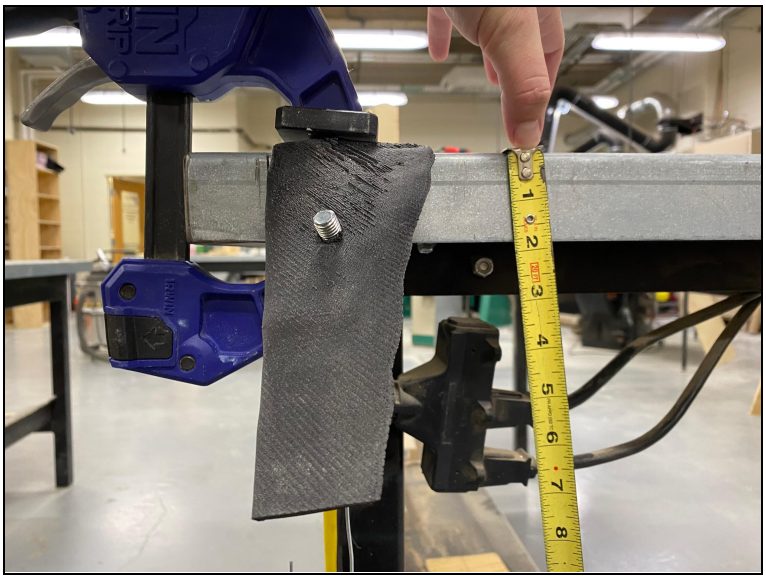

Figure 5: Deflection of Blades Exceeding 5in Found at 25lbs (111N)

The blades are connected to the rotor hub with 4-40 alloy steel screws, which possess a tensile strength rating of 170,000 psi. The maximum expected shear force on these screws due to the rotational forces during the competition is expected to be 47 psi. Wind tunnel testing was subsequently used to validate that the blades and rotor to ensure they are capable of withstanding the maximum levels of thrust, centripetal force, and shear force that will be encountered during the competition.

3.2. Blade Pitch

The 2022 team fabricated a custom active pitching system; however, the MaxVentus team identified areas where further improvements could be made. The 2022 design integrated the previously fabricated pitching system directly onto the drive train. Due to the linear bearing's contact with the high-speed rotating drive train exceeding 1200 RPM, excessive friction was introduced, negatively impacting the system's performance. To reduce friction between the linear bearing and the drive shaft of the turbine, a modification was made to the 2022 pitching system by incorporating a stainless steel sleeve within the linear bearing, as depicted in Figure 6. The linear and rotary bearing sizes and encasements were enlarged to accommodate the addition of this sleeve.

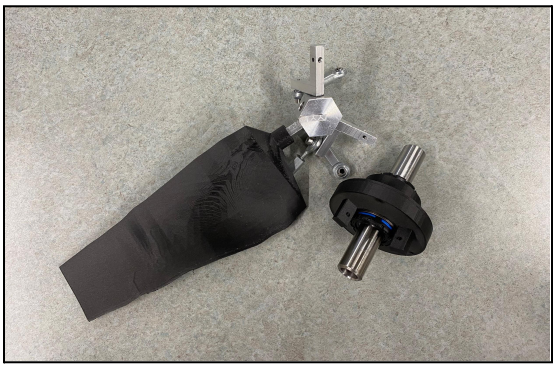

Figure 6: Proof-of-Concept Onyx Filament Blade and Pitching Components Incorporating Pitching Mechanics and Steel Sleeve

For dimensional testing purposes, parts were initially 3D printed, but the final components were fabricated from 6061 aluminum using a CNC machine to increase durability and reduce weight. To fabricate the linear bearing sleeve, a solid steel rod was bored to allow the ⅜" drive shaft to pass through. The outer diameter was machined to accommodate the linear bearing. The resulting hollow rod was then welded to a metal plate, which was subsequently fastened onto the nacelle's opening using 4-40 steel screws [Figure 7]. The sleeve successfully eliminated any contact between the drivetrain and the linear bearing while maintaining the normal functions of the pitching system.

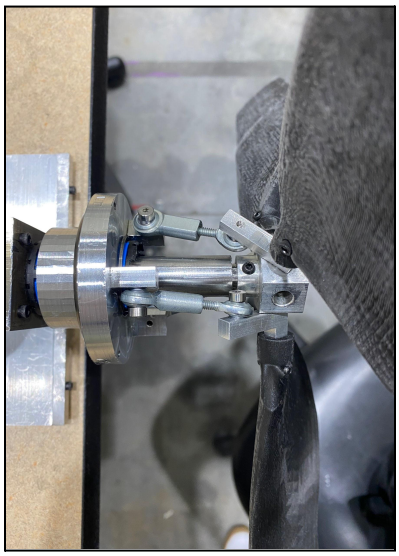

Figure 7: Fully Integrated Machined Pitching Components on Rotor and Nacelle

The implementation of the sleeve effectively addressed friction-related issues that were present in previous designs. Lastly, a wind sensor calibration was implemented, enabling the blades to actively pitch while in use, allowing for the blades' angle of attack to vary and reducing high thrust forces at higher wind speeds.

3.3. Rotor Fabrication

The blades and pitching components were fabricated on-site utilizing JMU's 3-D printers, which facilitated a streamlined and expeditious prototyping and testing process allowing for a quick turnaround of components. The aluminum pitching components were modeled using SOLIDWORKS and fabricated using an in-house CNC machine. The screw holes for both the blades and pitching mechanism were threaded for 4-40 screws. The selection of 6061 aluminum as the primary metal in the rotor was settled upon a multitude of factors, most notably its attributes such as convenience, lightweight nature, and non-magnetic properties.

4. Generator Design

After a thorough evaluation of various generator options, which included off-the-shelf DC motors and radial flux generators, MaxVentus opted to design and fabricate a 3-phase axial flux permanent magnet generator (AFPMG). This decision was based on several factors, including the generator's ease of fabrication, high power density, and ability to customize parameters to optimize power output with specific blades. To calculate the theoretical power output of the generator, the team utilized a mathematical model in MATLAB, which was refined by previous JMU competition teams. Throughout this process, critical parameters such as coil winding density, wire gauge, and magnetic air gap spacing were varied to determine their impact on the torque and rotational speeds required for the generator to produce a constant voltage when attached to different resistive loads. QBlade simulations of the rotor torque and rotational speed at each competition wind speed were then paired with the generator design simulations to identify steady-state operating points at each wind speed that resulted in maximum power production. From these simulations, a theoretical competition score, using the weights specified in the R&R, was estimated for each candidate generator design. This theoretical score was then used to facilitate the generator design selection process. The projected power-curve scores were estimated based on the score weighting criteria specified in the CWC 2023 Rules and Requirements document and can be found in Table 1. While a primary selection objective was to maximize the scoring potential, the team also had to select a design that would not exceed a maximum operating voltage of electronic components and not result in high rotational speeds. Although higher-scoring generator designs were identified, these designs potentially would exceed the 60 V electronics design limits or result in rotational speeds exceeding 1600 RPM.

Table 1: Generator Selection Process Using Theoretical Competition Scoring

Blade	Number of Wire Turns per Coil	Gauge of Wire	Theoretical Compeition Score
SA7024 TSR 3	200	28	50.08
SA7024 TSR 3	200	26	50.07
SA7024 TSR 3	175	28	50.28
SA7024 TSR 3	175	26	53.28
SA7024 TSR 3	150	28	49.85
SA7024 TSR 3	150	26	53.02
SA7024&FX-160 TSR 3	200	28	48.45
SA7024&FX-160 TSR 3	200	26	52.50
SA7024&FX-160 TSR 3	175	28	50.35
SA7024&FX-160 TSR 3	175	26	52.47
SA7024&FX-160 TSR 3	150	28	49.86
SA7024&FX-160 TSR 3	150	26	52.08

Using this pairing and selection method, a 3-phase wye configuration stator consisting of 9 coils and 175 wire turns of 26-gauge wire was identified for pairing with the previously described blade design.

The fabricated generator is a direct drive, three-phase, axial flux permanent magnet generator. It features nine coils that were wound within a 3D-printed mold, mechanically interconnected, and soldered in a 3-phase wye configuration. Additionally, the team enhanced the generator's structural integrity by applying fiberglass resin using the mold. Following the fabrication of the generator, the team conducted tests to validate the simulations. A dynamometer was used to measure the torque and rotational speed required to drive the generator at different constant voltages when connected to different loads. A speed-controlled DC motor was used to drive the AFPMG and a 2 Ω to 300 Ω potentiometer was used as the load. The team evaluated the generator's performance under varying motor speeds and resistances and compared the results to those predicted by the Matlab model. Readings of rotational speed and torque required for the generator to produce 12 V, 20 V, 30 V, and 45 V across four different load values were obtained. Figure 8 provides a comparison of the results (points) with the MATLAB model (lines).

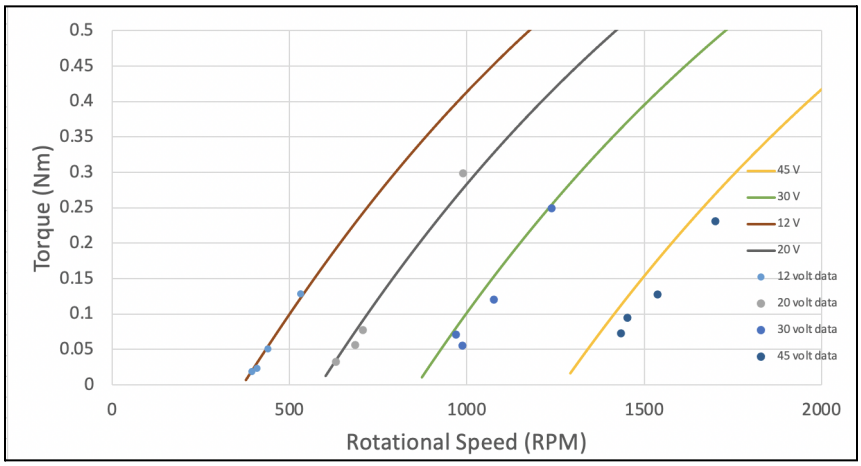

Figure 8: MATLAB Generator Model (lines) compared to measured (points) prototype generator characteristics

5. Structural and Foundational Design

Extensive research was conducted on various sand and sea-bed systems, including a gravity base, monopole, tripod, suction bucket, and jacket structures. After careful consideration, most of these were eliminated due to their weight, practicality, and difficulty of installment. A four-pile configuration connected to a 25.40cm x 25.40cm (10in x 10in) steel tamper plate structure with a welded 9.00cm tall, 3.81cm diameter pipe tower used as the lower tower such that the OPTP could firmly rest and be faceted onto was selected as the leading design. The tamper plate foundation was chosen to cover a large surface area within competition guidelines, minimize overturning moments, and resist settling or sinking due to vibration

The critical design challenge for MaxVentus' structure team was determining the optimal anchoring pile design to secure the foundation to the sandbed. Three conceptual designs were brainstormed, prototyped to scale using 3D printing, and subjected to a monopile tower cantilever static load test that simulated the forces the system would experience inside the wind tunnel (see Figure 9 for testing and prototype details). These three designs were developed by group research about common industry practices and standard methods to bury anchoring piles. Congruently, consultation with faculty who have structural/civil engineering backgrounds was conducted to gain insight and perspective on similar systems. The modified suction pile design

demonstrated the best resistance to overturning moment during the Proof of Concept test. Consequently, iterations of this design were prototyped and tested as well. From this test, the team gathered that all iterated designs performed similarly when subjected to the same test. As a result, the selection of the original suction pile design was based on two critical criteria: ease of installation and additional weight added to the foundation. Figure 10 shows results from both the PoC and Iteration Test.

Figure 9: 3D Printed Anchoring Pile Design Prototypes and Test Setup

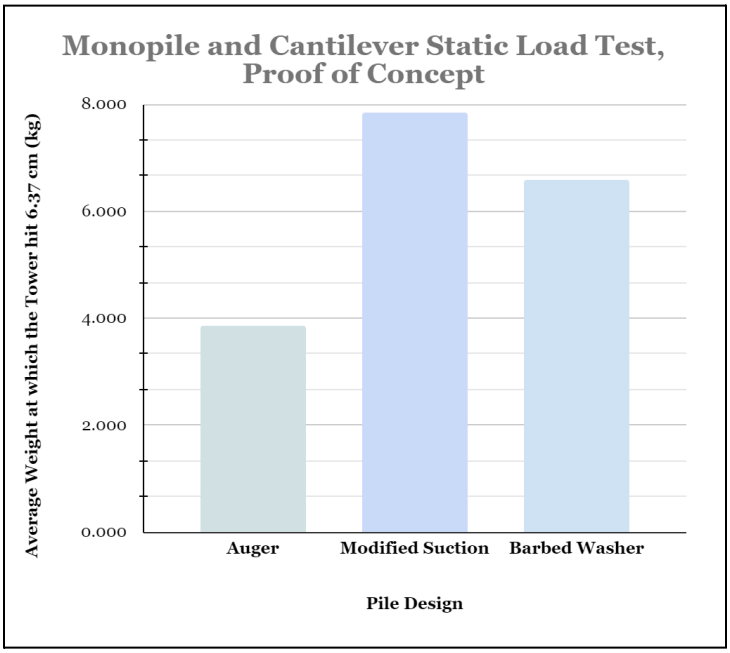

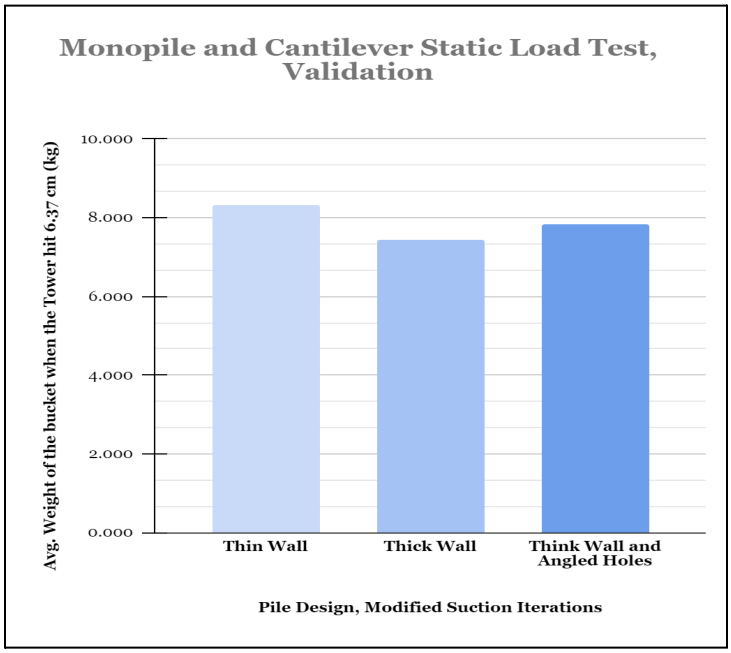

Figure 10: PoC and Iteration Test Results

After seeking expert guidance, the group modified the system's functionality by welding the piles to the foundational plate, improving connectivity and facilitating vibration distribution to the sand. The final design consists of four modified suction piles, each 13.34cm in height, welded onto the steel tamper foundation. A comprehensive view of the entirely fabricated foundational design is presented in Figure 11, and a technical drawing detailing the specifications of the subsystem is provided in Figure 12.

Figure 11: Fully Fabricated Foundation

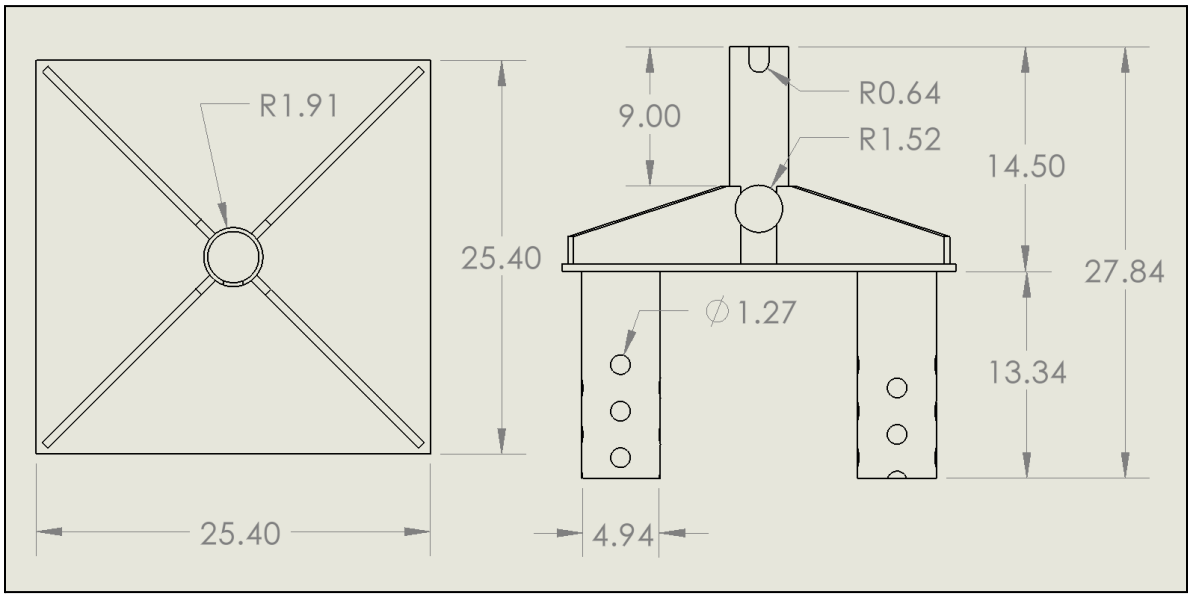

Figure 12: Technical Drawing of Foundation (units in cm)

The installation process utilizes a one-person driving method, with a team member placing the foundation into the sand and operating a sander tool with an attached 3D-printed

adapter piece capable of fitting in the lower tower to vibrate the structure into the sand. The sander with the adapter piece attached and step-by-step images of the installation process are depicted in Figure 13.

Figure 13: Installation Process and Sander Tool with 3D Printed Adapter Piece

As mentioned before, the structural components that would be inside the wind tunnel are all made of 6061 aluminum, excluding the wind sensor mount and nacelle cover which both were 3D printed. This design is largely continued from last year's wind turbine. Connected to the OPTP by three bolts is a base plate and tower sleeve securing a 54.45cm hollow pipe with an outer diameter of 3.81 and an inner diameter of 3.77cm used as the upper tower. The nacelle is supported and rotated by a flange that has been welded to the upper tower's top, effectively positioning the rotor hub at a height of 60cm from the base of the wind tunnel. After installation, the rotor can be aligned with the upwind direction and secured in place. Subsequently, a secondary plate below the flange and the nacelle's bottom plate generate a compressive force on the flange when fastened with three screws. The upper tower and the supporting components including the wind sensor mount can be seen in Figure 14.

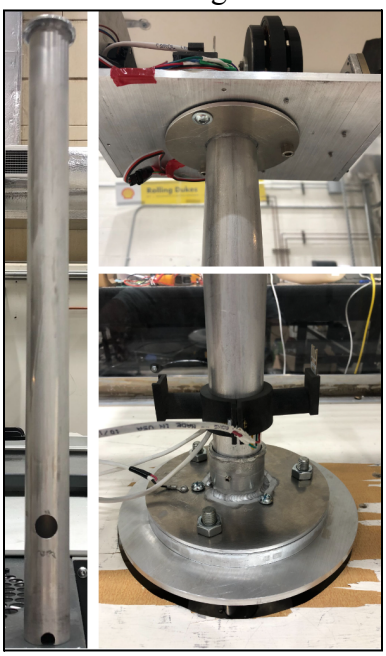

Figure 14: Upper Tower and Supporting Components

6. Nacelle Design

The drive train is supported by 2 rotary bearings that go through the nacelle. The nacelle houses 2 linear actuators, the AFPMG, emergency disc brake, encoder, and rectifier. One linear actuator moves the pitching system back and forth adjusting the pitch of the blades. The other linear actuator pulls the brake cable deploying the emergency brake when prompted. This can be seen in Figure 15.

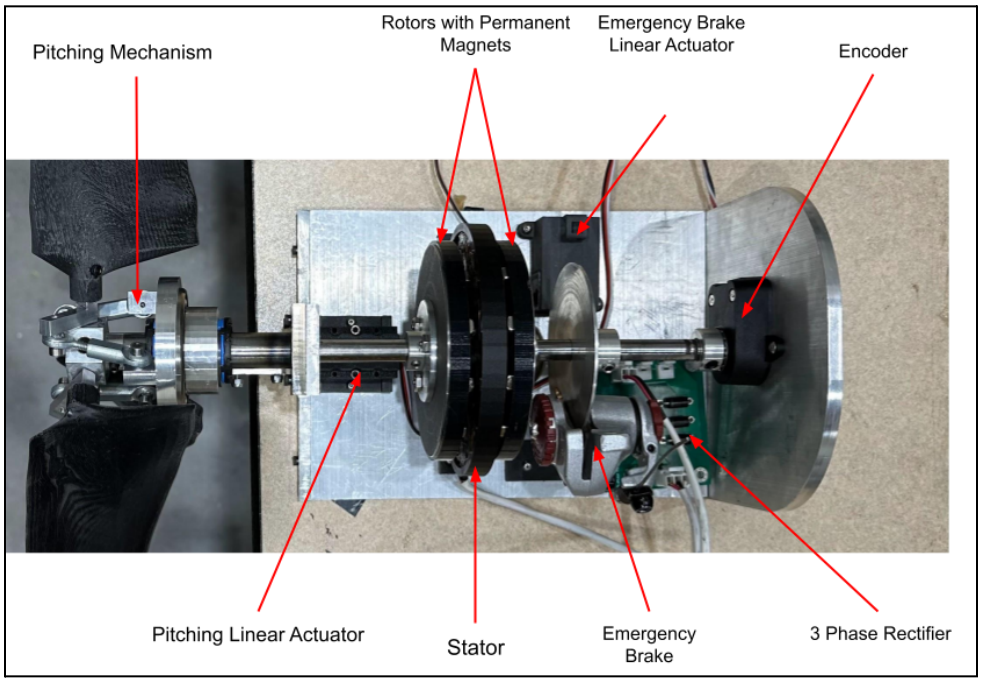

Figure 15: Labeled Components of Nacelle

The MaxVentus team successfully designed a 3-D printed shell, as depicted in Figure 16, aimed at encapsulating the delicate nacelle components, such as the drivetrain and wires, while simultaneously mitigating the aerodynamic drag imposed on the system as a whole.

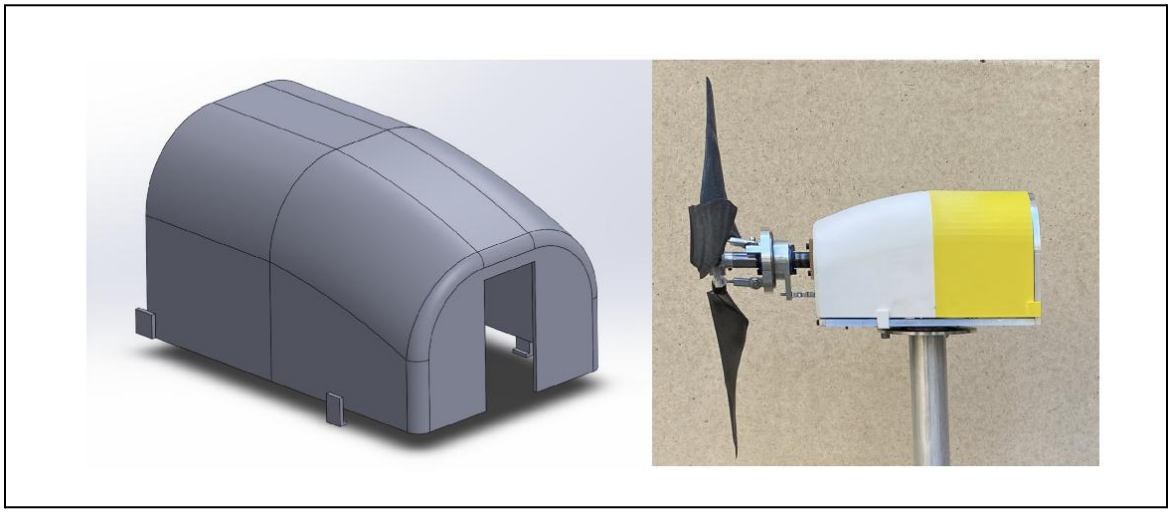

Figure 16: SOLIDWORKS Model Alongside Fabricated Nacelle Cover

To achieve this design objective, the front aluminum plate underwent alterations to accommodate the securement of the shell, ultimately leading to a reduction of 9 square inches in the frontal flat surface area of the nacelle. The implementation of this feature yielded a noticeable decrease in both the thrust forces on the nacelle and the overturning moment applied to the foundation.

7. Electronics and Controls

The MaxVentus team employed benchmarking to evaluate previous designs as a reference point in the decision-making process for hardware and controls, as illustrated in the accompanying diagrams. The electronics and control subsystems' main purposes are to receive unregulated power from the generator, regulate and distribute that power, since the operating state of the turbine, and control the operation of the turbine. Unregulated three-phase power is regulated with a Schottky diode bridge rectifier. A wide-input buck-boost converter is used to regulate the rectified power to a constant voltage level for the entire system. From there, the electrical system distributes the regulated power to the control system and the load. A microcontroller is used to gather feedback from a rotational speed sensor, a wind speed sensor, and current and voltage sensors to determine the operational state. A digitally controlled resistive load is used to perform maximum power point tracking. At wind speeds below 11 m/s, the control algorithm will optimize power production. Above 11 m/s, a linear actuator is used to modify the blade pitch angle to reduce thrust and produce rated power. A diagram of this system’s energy flow can be seen below in Figure 17. Based on competition rules and requirements, the energy stored in this electronics system cannot exceed 10 Joules of energy and this system meets that with a total of only 0.3 Joules stored. Considerations were taken into account for other methods of controlling rated power output including transmissions, friction braking, and flap control. However, the complexity and control difficulty as well as the extra cost associated with these concepts resulted in their elimination.

The sub-teams primary focus for the controls was on improving the blade pitching response time. This involved leveraging the existing hardware infrastructure set in place by the previous year's team due to cost and logistical constraints while enhancing the control algorithm using Arduino IDE instead of C++, which involved trade-off analysis. A diagram of the control algorithm’s decision-making logic can be seen below in Figure 18. To achieve this objective, the electronics subteam conducted comprehensive research and identified relevant MATLAB and Simulink models for wind turbine control systems, which are currently utilized as a reference for the control system. By incorporating these models and performing tests, the team input variables from generator and blade system simulations to assess the system's performance under varying wind profiles. Multiple power curves and equations, depicted in the figures below, were derived by testing the turbine at various wind speeds and determining the point of maximum power output when increasing the load on the turbine. The curve shown in Figure 19 is the measured load control curve for the prototype. The line of best fit is used to determine the load setting during operation. If the observed RPM is greater than what is expected for the power produced (above the line), then the controller increases the load or decreases resistance to slow the rotor. If it is less than expected (below the line), it increases the resistance or decreases the load to try to speed it up. The units here are 10 times the RPM for rotational speed and Centiwatts of power in

order to limit the number of characters transmitted through the serial monitor in the Arduino IDE code.

Calibration and calculations will be required at the competition due to the environmental variations and the constraints imposed by our wind tunnel since we can only test up to about 8 or 9 m/s. Therefore, the team must fine-tune the system's controls to optimize performance during testing. From there, the team can program the equation of the line of best fit into the Arduino IDE code and fully automate the pitching and braking actuators based on the wind speed.

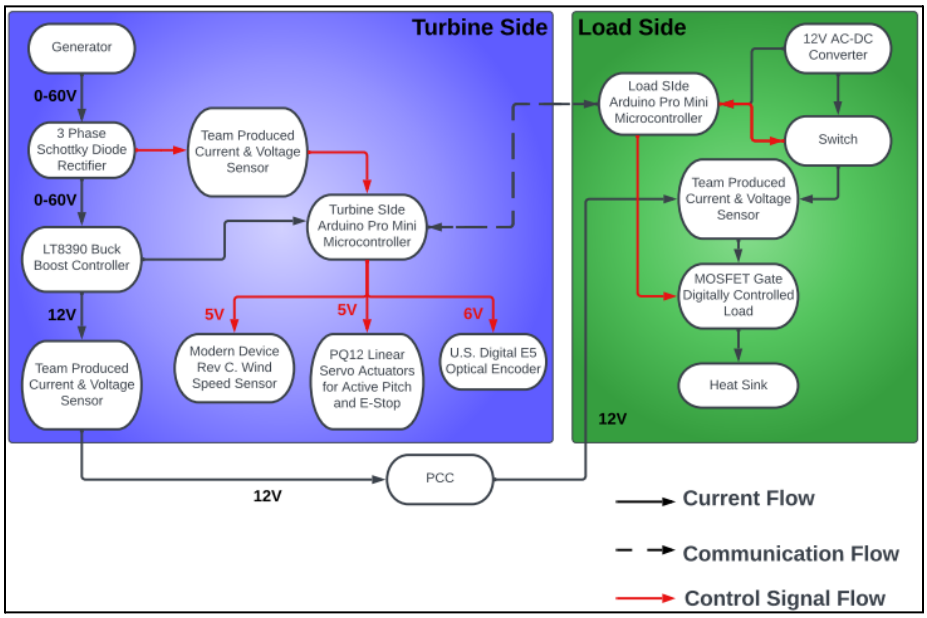

Figure 17: Electronics System Schematic and Energy Flow

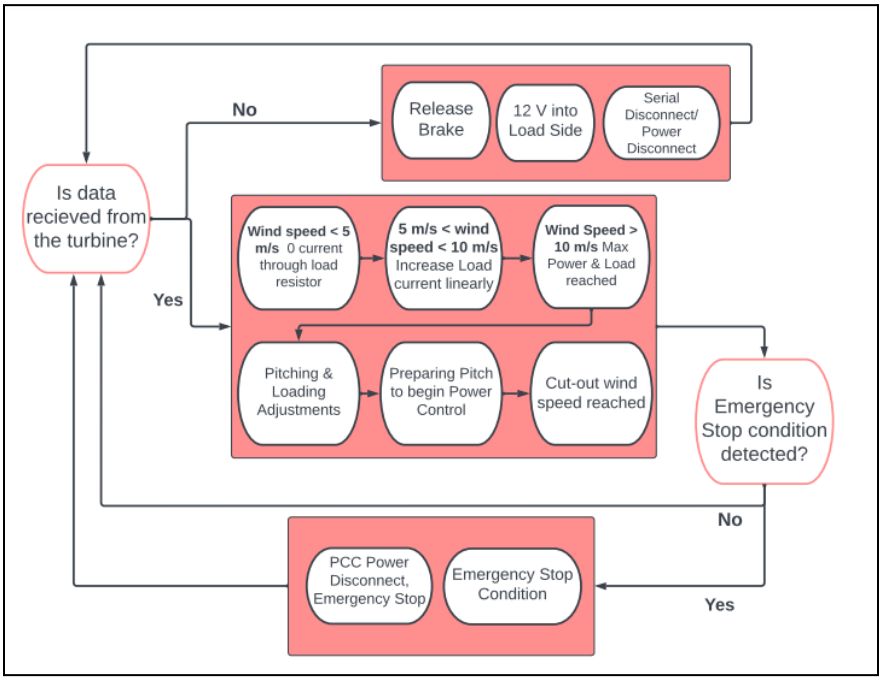

Figure 18: Control System Decision-Making Logic

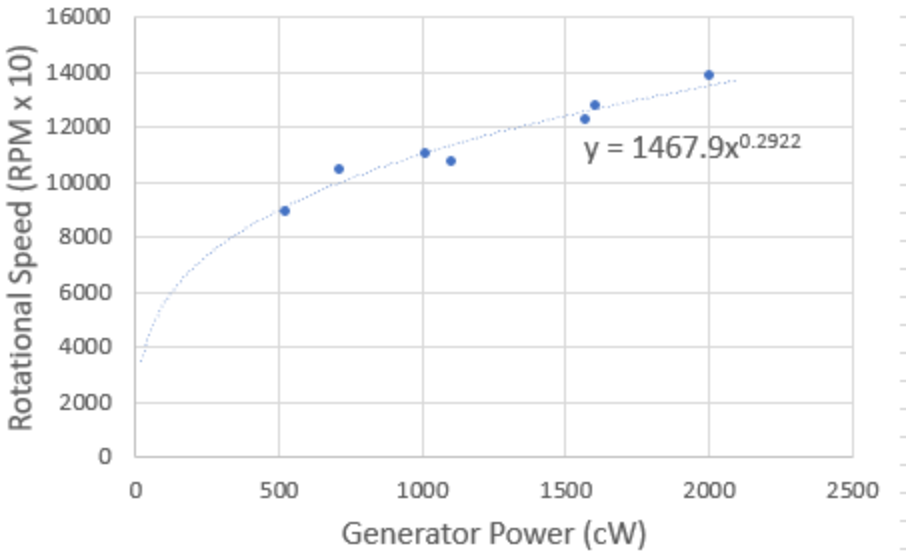

Figure 19: Power Control Curve and Equation

8. New for 2023 Design

JMU's success in the previous year's Turbine Design Contest prompted MaxVentus to identify potential areas for improvement. Similar design decisions to previous years, including those pertaining to generator and blade design, as well as the electronics system, were made. While generator parameters and blade designs differed from prior years, the team used a comparable design process that involved utilizing QBlade and MATLAB to make design decisions. With sourcing constraints and the previous team's achievements in mind, MaxVentus decided to reuse most of the electronics system. However, the team focused on improving the code from the previous year. An area of primary concern was the structure subsystem, which was the main source of failure for the prior year's team. To address this issue, the team designed a flat-plated, four-pile anchoring system, ruling out a suction bucket and gravity base. All design methods and justifications are further elaborated upon in their respective sections of the report.

Moreover, MaxVentus identified areas for improvement in the previous year's design. The custom active pitching mechanism used by the previous team was successful, but not without its flaws. The drivetrain and linear bearing exhibited friction that impacted the rotor's overall efficiency. To address this issue, the team incorporated a stainless steel sleeve to act as a boundary between the drivetrain and linear bearing. This modification successfully addressed the previous design's fault and improved the efficiency of this year's design. Based on the data from last year that described where the foundation encountered significant pressure in one direction, and where the team’s foundation and anchoring system saw failure, there was a strong inclination to start the foundation and anchoring system from scratch. Consequently, the team's main objective was to cover a substantial surface area of the sand bed to resist overturning moments effectively. Moreover, the team identified that a four-anchoring pile design would provide a robust overturning resistance applicable on a large scale. This design aimed to exhibit strength in any direction of the wind's blowing. The challenge for MaxVentus' Structure team was to determine the optimal pile design to anchor the foundational plate firmly onto the sand bed.

9. Full Turbine Assembly

The successful assembly of the full turbine system was accomplished through continuous communication and interdependence between subsystems, including the rotor, electrical, and structure/foundation. Prior to integration into the entire system, each subsystem was tested independently to ensure that desired output, results, and performance were achieved. The team was able to meet most competition requirements and completed testing in JMU's wind tunnel.

However, due to limitations of the JMU wind tunnel, wind speeds exceeding approximately 10 m/s were not attainable during testing. Nonetheless, comprehensive calibration and performance measurements were made during wind tunnel testing to evaluate the fully assembled prototype systems optimal operation. Figure 20 shows the predicted and measured power curve performance for the MaxVentus prototype. Based on measurements of the power produced at the generator, the rotor appeared to perform slightly better than predicted with the Qblade models, exhibiting a C_p of 0.46. Simultaneous power measurements at the load (or PCC) indicated an electrical conversion efficiency of approximately 75% , with losses incurred due to stator winding and wire length resistance and DC-to-DC converter losses. The purple line in Figure 20 indicates a maximum of 41 W delivered to the load at 11 m/s wind speeds. However, power production is expected to be reduced at the competition due to the reduced air density in Boulder, CO when compared to Harrisonburg, VA.

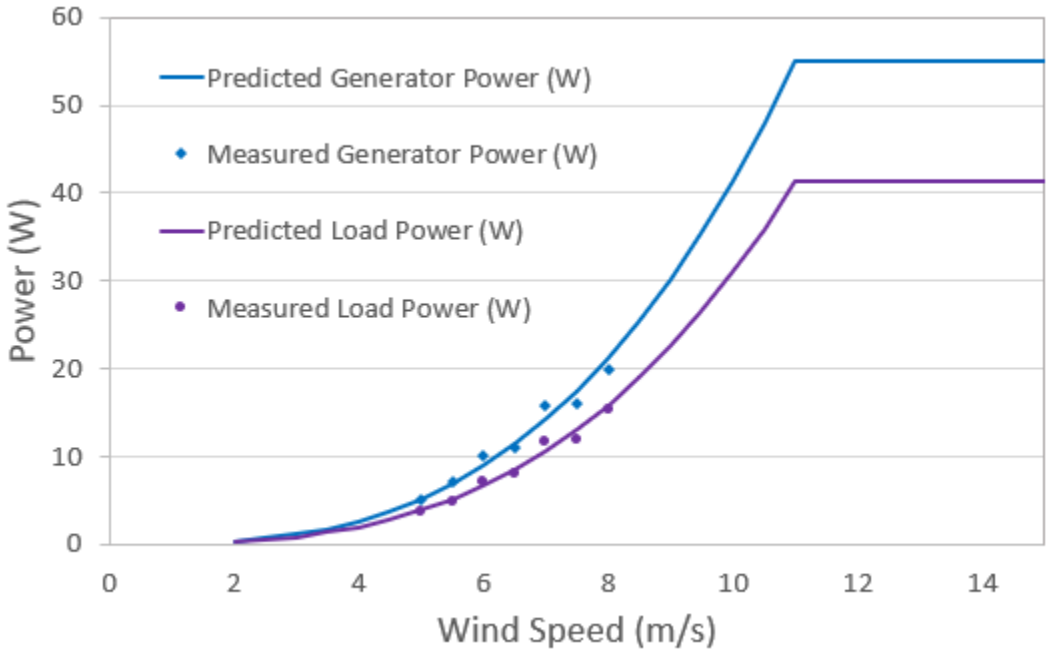

Figure 20: Measured vs. Predicted Generator & Load Power Curves

9.1. Safety Inspection

Throughout the entire turbine fabrication process, the team underwent several safety inspections to ensure compliance with competition regulations. Dr. Keith Holland conducted multiple safety inspections, both prior to and subsequent to the full turbine assembly, to guarantee its safe utilization and efficacy in the wind tunnel. Moreover, the team was able to

enlist the help of the master electrician, Scott Weeks, an Engineering Technician. Mr. Weeks was able to conduct the Safety and Technical Inspection Sheet, as given in Appendix C of the R&R, to further verify the safety and performance of the turbine.

9.2. Cut-in Wind Speed

Following extensive wind tunnel testing and component fine-tuning, the team found that the power output could initiate production at an approximate velocity of 4.4 m/s, subsequently generating power consistently at approximately 4.6 m/s. It is the team's belief that by implementing the active pitching mechanism, the blades could be effectively feathered from the onset, thereby enabling a lower cut-in speed, and adjustably pitched up to 0° pitch to optimize performance beyond 5 m/s.

9.3. Safety Task

In accordance with the relevant R&R, the turbine assembly has been designed to incorporate all required safety measures. Notably, the turbine has undergone intensive testing and has been demonstrated to halt entirely within a span of 5 seconds upon activation of the E-stop shutdown button. Following the disengagement of the E-stop, the turbine was observed to restart seamlessly, subsequently resuming optimal power generation.

10. Prototype Testing Commissioning Checklist

A comprehensive assembly checklist, detailing all crucial steps required for seamless and appropriate turbine assembly, is presented in Table 2 for adherence by all participating team members during the competition. The checklist encompasses all vital tasks necessary for efficient operation and comprises designated team members assigned to complete each task, as well as verify its proper execution.

Table 2: Checklist for Assembly and Verification of Wind Turbine

Verification Step	**Initiating Team Member Initials**	**Verification Team Member Initials**
Gather foundation and insertion materials	JS	BL
Feed electrical cables through the base plate and foundation structure	JS	BL
Fasten the base plate to the sand bed	JS	BL
Vibrate the base plate into position until the surface is flush with the sand surface	NG	AZ
Ensure levelness of sand bed	NG	AZ

foundation		
Attach transition stub	NG	AZ
Move the foundation tub underneath the wind tunnel	NG	AZ
Connect necessary wires from the nacelle to the foundation connection point	JS	AZ
Fasten and secure the turbine base plate and ensure the wind sensor is in the direction of incoming wind	JS	AZ
Ensure the nacelle is properly faced and fastened to the lock place	YS	NG
Connect all necessary wires from the tower to the turbine controls	JS	AZ
Connect power from PCC to load and verify the connection	AZ	JS
Connect and verify communications cable	JS	AZ
Plug the AC/DC adapter into an outlet and verify the power	YS	NG
Run a test of E-stop and verify activation	AZ	JS
Disengage E-stop	AZ	JS
Verify cut-in wind speed	AZ	JS
Verify correct wind speed measurements	AZ	JS
Verify the proper voltage and current output readings	AZ	JS
Confirm RPM readings	AZ	JS
Alert judges to commence the testing sequence	BL	NG